Analysis of Inter-modulation Products and Nonlinear Distortion in RF OFDM Transmitter Systems

Máirtín O'Droma
Department of Electronic and Computer Engineering
University of Limerick
Limerick, Ireland
mairtin.odroma@ul.ie

Yiming Lei
Department of Electronic and Computer Engineering
University of Limerick
Limerick, Ireland
yiming.lei@ul.ie

Eduard Bertran
Department of Signal Theory and Communications
Universitat Politècnica de Catalunya. Barcelona, Spain
bertran@tsc.upc.es

Pere Gilabert
Department of Signal Theory and Communications
Universitat Politècnica de Catalunya. Barcelona, Spain
plgilabert@tsc.upc.es

***Abstract*—Orthogonal Frequency Division Multiplexing (OFDM) systems are significantly sensitive to the nonlinear distortion caused by RF power amplifiers. Generally, nonlinear distortion of OFDM signals, which generates a huge number of inter-modulation products (IMPs), is treated as a macro phenomenon. In this paper, low order IMPs are classified into various categories by their composition and the characteristics of IMPs in each category is presented. Relationships between single IMP and nonlinear distortion are also explored. The popular Bessel-Fourier (BF) envelope model with associated three signal representation approaches are used as analysis tools. An IEEE 802.11a signal is used and the nonlinear envelope is measured from a GaN power amplifier.**

***Keywords*-nonlinear distortion, power amplifier, OFDM, IMP**

I. INTRODUCTION

OFDM technology is now an established attractive digital modulation scheme for modern wireless communication systems, e.g., [1, 2]. OFDM systems, however, generally have a high peak to average power ratio (PAPR) as they may consist of large numbers of independent sub-carriers modulated with adaptive multi-level quadrature amplitude modulation (QAM) schemes. Thus OFDM systems are very sensitive to the nonlinearity of RF transmitters, and the power amplifier (PA) is the main source of nonlinear distortion. Furthermore, the operating point of PAs may have to be driven into the highly nonlinear range due to the need for better power added efficiency (PAE), since the PA consumes most power in the transmission process, [3, 4]. In practice nonlinear distortion produces a huge number of IMPs in and around the fundamental OFDM signal band and, theoretically, in all harmonic bands, [5, 6]. The IMPs within the fundamental band are the focus of this nonlinearity analysis, since harmonics and IMPs at harmonic frequencies may be removed from the output signal by filters. The IMPs within the fundamental band impair the signal modulation fidelity, e.g. as measured by Error Vector Magnitude (EVM), and also causes interference in adjacent channels, which is measured by the output spectrum mask, [7].

Due to the complexity of such distortion, comprising lots of IMPs and having a noise-like characteristic, it may be effectively treated as a macro phenomenon, e.g., [8, 9]. Complementary to and informative for this approach is an analysis which delves more into the composition of the IMPS, their distribution densities and their behaviour as a function of the level of nonlinearity. Aspects of this analysis are undertaken in this paper. Our approach is to classify IMPs into various categories by their composition. Here the characteristics of IMPs in each category, including distribution density functions and the power behaviour of each single IMP, is presented, along with their relationship to the level of nonlinear distortion.

Memoryless PA nonlinear distortion only is treated here. The popular Bessel-Fourier (BF) is chosen for the PA behavioural modeling, for its accuracy, extensibility, and unique decomposability when handling multicarrier signals, [4, 10]. An appropriate signal representation technique has to be selected also.

Device measurements, the AM-AM and AM-PM characteristics, are those extracted from a GaN PA operating at 2.15 GHz. The AM-AM may be seen in Fig. 1. Here the input and output are expressed as the back off from the corresponding saturation power. This saturation power is defined as where the derivative of the output gain first reaches 0.1, [12].As it happens the AM-PM distortion is negligible over the dynamic range of interest [11]. The signal modelled is an un-coded IEEE 802.11a OFDM signal with 16-QAM applied.

II. BESSEL-FOURIER MODEL AND EXAMPLE PA ENVELOPE

Letting the PA's measured AM-AM and AM-PM conversions of the envelope of the fundamental band be denoted as $g[.]$ and $\Phi[.]$, the general form the output, $s_0(t)$, may be written as:

$$s_o(t) = \frac{g[A(t)]}{A(t)} \cdot e^{j\Phi[A(t)]} \cdot s_i(t) \qquad (1)$$

where $s_i(t)$, the complex analytic form of the input, is

$$s_i(t) = A(t) \cdot e^{j\phi(t)} \tag{2}$$

Applying the BF model to the PA, the output envelope of the fundamental band may be expressed as a linear sum of finite Bessel series terms of the first kind, J_n, that is, [10],

$$g(A(t)) \cdot e^{j\Phi[A(t)]} = \sum_{k=1}^{L} b_k \cdot J_n(\alpha k A(t)) \tag{3}$$

where α is a parameter related to the model's dynamic range, and b_k are the model coefficients. In this case n is one, as the envelope signal is presumed to be that of a single carrier. The coefficients may be obtained by a fitting process, by which the errors between measured values and modelled ones are minimised.

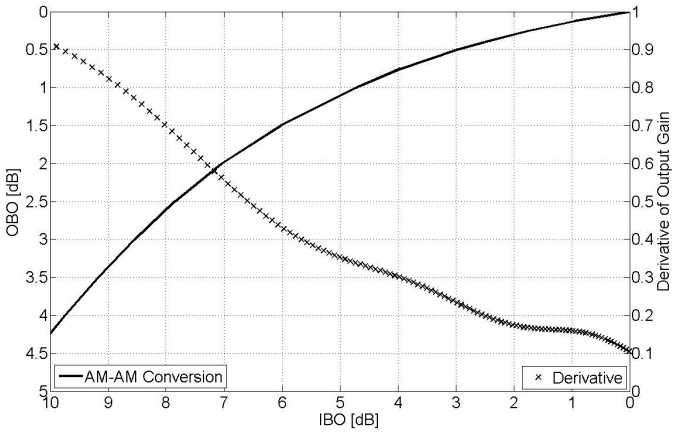

Fig. 1. AM-AM conversion & first-order derivate function of output gain of measured envelope characteristic from the example GaN PA at 2.15GHz.

III. ANALYSIS OF IMPS BY COMPOSITION

The MFTD signal representation approach, [14], is the means to enable this analysis. It's the multicarrier form of the Bessel Fourier model in which the generated IMPs are calculated and tracked individually. The M-symbol OFDM input signal may be written [4 & 14]:

$$s_i(t) = \sum_{s=1}^{M} \sum_{l=1}^{N} A_{l,s} \cdot e^{jn_l[\omega_l \cdot (t - sT) + \phi_{l,s}]} \tag{4}$$

where $A_{l,s}$ and $\phi_{l,s}$ are the amplitude and phase respectively of the l^{th} OFDM subcarrier of angular frequency ω_l in the s^{th} OFDM symbol having symbol duration T. Notably $A_{l,s}$ may remain unchanged for some adjacent OFDM symbols. The PA output for this signal may be shown to be:

$$s_o(t) = \left[\sum_{k=1}^{L} b_k \sum_{\substack{n_1, n_1, \ldots n_N = -\infty \\ \sum n_l = 1}}^{\infty} \left\{ \prod_{l=1}^{N} \left[J_{n_l}(\alpha k A_l(t)) \right] \cdot e^{j \sum_{l=1}^{N} n_l \cdot [\omega_l t + \phi_l(t)]} \right\} \right] \tag{5}$$

where J_{nl} denotes the n_l^{th} order term of a Bessel function of the first kind. It comprises, besides the fundamental output components, all the harmonics and IMPs over all bands.

The value of $\sum_{l=1}^{N} n_l$ for any combination of n_l, $l=1, 2, \ldots, N$ denotes the harmonic level of any IMP. Hence the fundamental band components (including wanted and distorted components) are selected by setting the condition $\sum_{l=1}^{N} n_l = 1$. Within this band, or within any band for that matter, the IMPs of any order γ are selected by setting the condition: $\sum_{l=1}^{N} |n_l| = \gamma$.

With this the IMPs are generated their defining parameters calculated individually, with each IMP mapping onto a unique realisation of the parameter set $\{n_l\}$ in equation (5). Besides harmonics and orders, it is possible to further classify IMPs by subcarrier composition defined by values of non-zero elements in the set $\{n_l\}$. The dominant lower order 3rd and 5th IMPs in the fundamental band may be classified into 2 and 6 composition types, respectively, as given in Table I, in which only non-zero $\{n_l\}$ values are presented. In the analysis below, the IMPs in the fundamental band are our focus, and IMPs at higher order harmonics are ignored.

TABLE I: Subcarrier composition types of 3rd and 5th order IMPs at fundamental band

Type	$\{n_l\}$	Type	$\{n_l\}$
3A	(2, -1)	**5C**	(2, 1, -2)
3B	(1, 1, -1)	**5D**	(1, 1, 1, -2)
5A	(3, -2)	**5E**	(2, 1, -1, -1)
5B	(3, -1, -1)	**5F**	(1, 1, 1, -1, -1)

From the MFTD approach, it may be shown that the distribution density functions (DDFs) in the frequency domain of the IMPs of various types are frequency-dependent (i.e. on the subcarrier frequency), but independent of both the PA characteristics and the operating point. The DDFs of all 8 types of 3rd and 5th orders, listed in Table I, arising from the application of a 802.11a signal comprising 52 sub-carriers and a null DC subcarrier to a nonlinear PA, are shown in figure 2.

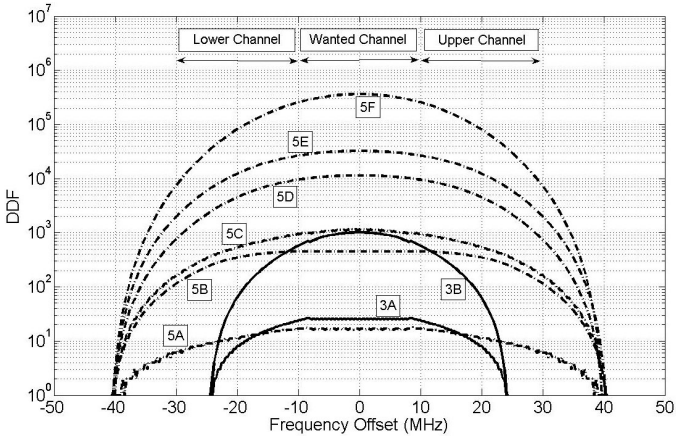

Fig. 2. DDFs of all IMP types of 3rd and 5th orders over the frequency domain

As would be expected, the IMP types 3B and 5F, composed of higher numbers of contributing subcarriers – i.e., of higher complexity, have relatively higher-valued DDFs. This may be seen in the DDF graphs in figure 2. The peak value of the DDF of type 5F is around 300 times higher than that of type 3B.

In the MFTD signal representation approach, the relationship of the power of a single IMP to both the operating point and its composition is made visible. The estimated power of a single IMP of all 8 types over a large dynamic range is shown in figure 3. For this estimation, the amplitudes of all input subcarriers are here assumed equal. The reference powers used in the normalisation at each operating point is the output power at that point.

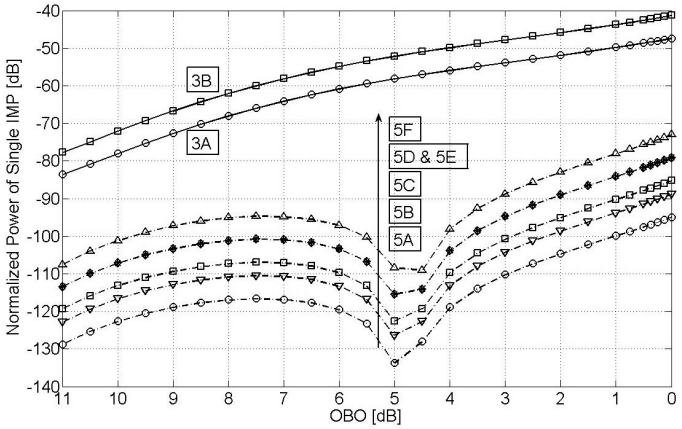

Fig. 3. Normalised powers of single IMP of all types in Table I.

The IMP behaviour in figure 3 indicates that with an increase of input power the ratio of the power of a single IMP to total output power increases, implying an increase in signal degradation as the operating point moves towards the saturation point. This is in fact the case. Another observation is that the power of the single IMP of two types, 5D and 5E, are identical over the whole dynamic range. That this is not actually an 'accident' may be explained. Considering:

$$J_{-n}(x) = (-1)^n J_n(x) \tag{6}$$

we may have

$$[J_1(\alpha s A)]^3 \cdot J_{-2}(\alpha s A) = [J_{-1}(\alpha s A)]^2 \cdot J_2(\alpha s A) \cdot J_1(\alpha s A) \tag{7}$$

Applying (7) to (5), we may show that the power ratio of a single IMP of type 5E to that of a single IMP of type 5D is 1. It may also be seen that the ratios between the power curves of single IMPs of various types of one order vary little, just several dB, over the dynamic range of interest. This is not an 'accident' Either but may be explained with the same argument. A key finding from figure 3 is that IMPs of types with relatively higher complexity also have higher power level.

As the AM-PM conversion of this GaN PA may be neglected, the coefficients of the BF model may be regarded as real numbers and their phases (5), expressed as:

$$\begin{aligned}\theta(t) &= \sum_{\substack{n_1,n_1,\ldots n_N=-\infty \\ \sum n_l=1}}^{N} n_l \cdot [\omega_l t + \phi_l(t)] \\ &= \sum_{\substack{n_1,n_1,\ldots n_N=-\infty \\ \sum n_l=1}}^{N} [n_l \omega_l t] + \sum_{\substack{n_1,n_1,\ldots n_N=-\infty \\ \sum n_l=1}}^{N} [n_l \phi_l(t)], \qquad = \theta_f(t) + \theta_p(t)\end{aligned} \tag{8}$$

where $\theta_f(t)$ indicates the angular frequency of the IMP, and $\theta_p(t)$ is its phase. In order that the phase of the IMP may be considered as a quasi uniform-distributed random variable over a phase range from zero to 2π, the probability distribution function of the phase of a single IMP may be regarded as an operating-point independent variable.

A conclusion from this analysis of the individual IMP's phase value, is that the PA mainly affects the power of single IMPs rather that its phase, i.e., that the DDFs and phase characteristics of single IMPs are PA independent. To sum up, from figures 2 and 3, it is clear that IMPs of type 3B and 5F have the highest DDF and the highest single IMP power among IMPs of their order and type and they actually dominate the 3rd and 5th order nonlinear distortion, respectively. So we may use IMPs of type 3B and 5F to approximately represent the 3rd and 5th order nonlinear distortion components, respectively.

IV. ANALYSIS OF NONLINEAR DISTORTION

The PA output signal includes the wanted output signal and the distortion output signal. Both can be treated as complex Gaussian processes. Figure 4 shows the simulated probability distribution (bars) of the magnitude of that part of the distortion component in the fundamental subcarriers frequency band. The distribution was obtained using around 100 FFT OFDM symbol frames. The PA operating point is at 4.5dB output back-off (OBO). The solid curve represents a Rayleigh distribution function, which is the theoretical probability function of the magnitude of a zero-mean complex Gaussian process. The results clearly show a good fit bars obtained by the simulation to the theoretical.

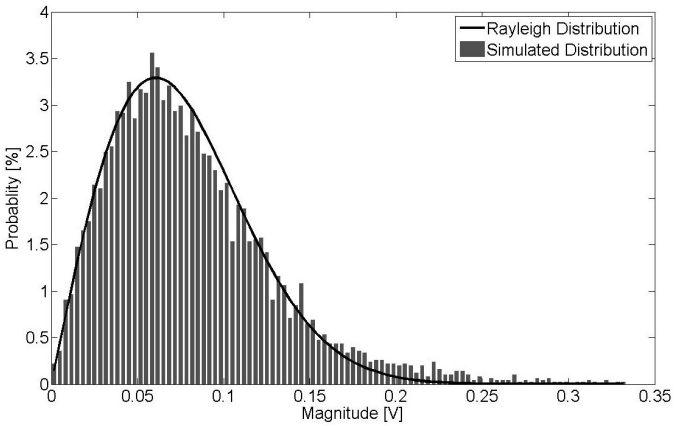

Fig.4. Probability distribution of the magnitude of nonlinear distortion component in the fundamental subcarrier band for the PA at 4.5dB OBO with 100 FFT/IFFT OFDM symbol blocks considered. The bars are simulated data, and solid curve is the Rayleigh distribution.

In figures 5a and 5b, the power spectral masks of low-order output components (including wanted, 3rd, 5th, 7th and 9th components) at both 3dB and 0.5dB OBO are presented. The DTD signal representation approach, [14], provides a spectral mask for the total output signal in figures 5a and 5b, which shows very good consistency with the spectrum of wanted and 3rd order components obtained by Stat signal representation approach, [14].

As analysed above, the IMPs of types 3B and 5F dominate the nonlinear components of 3rd and 5th orders, respectively. From figures 2 and 3, we may know the peak value of DDF of IMP type 5F is around 300 times (around 25dB) higher than that of type 3B, but the power of a single IMP of type 3B is

higher than that of a single IMP of type 5F by around 30-50dB over the whole dynamic range. As mentioned above, we may use IMPs of type 3B and 5F to approximately represent the 3rd and 5th order nonlinear distortion components and so the power of 3rd order nonlinear distortion is around 5-25dB higher than the power of 5th order nonlinear distortion. That is why, generally, the 3rd order component dominates the nonlinear distortion.

From figure 3, we can see that the gap between the powers of single IMPs of types 3B and 5F is about 40dB at 3dB OBO, so the gap between the masks of 3rd and 5th order distortion at the DC subcarrier should be about 15dB, since the gap of DDFs of type 3B and 5F is about 25dB there, as given in figure 5a. The power spectral masks of output components at 0.5dB OBO is presented in figure 5b, and we can see that the gap between the masks of 3rd and 5th order distortion at DC subcarrier is only about 7dB, since the power gap between a single IMP of types 3B and 5F is only 32dB at 0.5dB OBO. It is notable that the influence of the 5th order nonlinear distortion can not be neglected at an operating point of 0.5dB OBO.

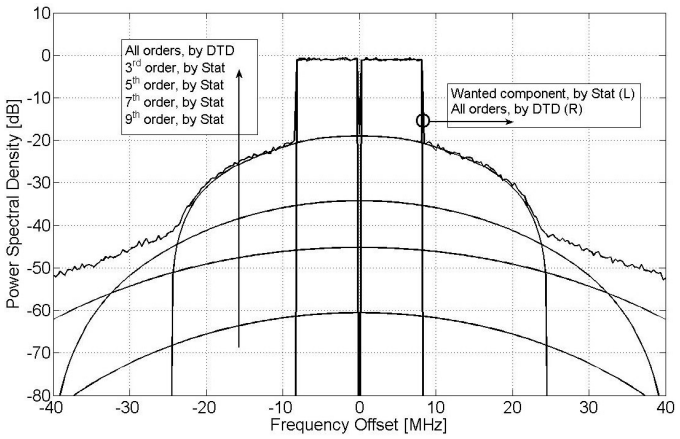

Fig. 5a. Power spectral masks of the total output (by DTD), wanted components, and low-order nonlinear distortion components (by Stat); the operating point is at 3dB OBO.

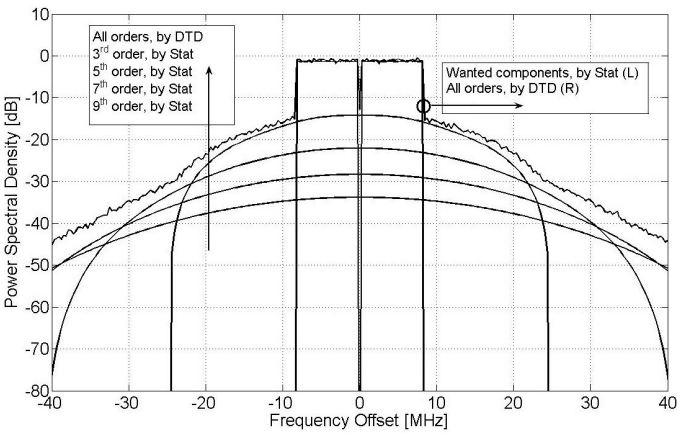

Fig. 5b. Power spectral masks of the total output (by DTD), wanted components, and low-order nonlinear distortion components; the operating point is at 0.5dB OBO.

CONCLUSION

In this paper, how the investigation of the composition and characteristics of IMPs arising in nonlinear amplification of OFDM signals through RF nonlinear power amplifiers is possible is presented. This makes possible the direct analysis of the actual IMPs generated in any nonlinear PA, and provides different and additional information to usual statistical analysis alone.

IMPs are classified according to composition into various categories, and distribution density functions and power spectral density functions of these categories are found and presented. From this it was shown that IMPs of certain categories will dominate the total IMP distortion. This is a useful insight. It also has implications for the individual subcarrier power distribution and power distribution algorithms used in OFDM systems and which are generally focused on PAPR minimisation.

In support of this analytic approach to IMPs, the paper includes an initial investigation of the statistical characteristics, as a function of composition and category, of the actual 3rd and 5th order IMPs generated when an IEEE 802.11a OFDM signal is amplified by a GaN PA.

ACKNOWLEDGMENTS

The authors wish to acknowledge support from Dr. Bernd Bunz and Prof. Gunter Kompa, University of Kassel, Germany, in providing the measurements of the GaN power amplifier used in this paper. •The authors also wish to acknowledge the support from Telecommunications Research Centre, University of Limerick, Ireland; TARGET, a European Union FP6 NoE (IST-1-507893-NOE); SFI (Ireland) and IRCSET/EMBARK Research Scholarship; Spanish Ministry of Science and Innovation (CICYT- research project TEC2008-066684-C03-03); Department of Signal Theory and Communications, Universitat Politècnica de Catalunya, Barcelona, Spain

REFERENCES

[1] M. O'Droma and I. Ganchev. "Toward a ubiquitous consumer wireless world". *IEEE Wireless Communications*. Volume 14, Issue 1, Feb. 2007 Page(s): 52 – 63

[2] Ming Jiang and L. Hanzo. "Multiuser MIMO-OFDM for Next-Generation Wireless Systems". *Proceedings of the IEEE*, Volume 95, Issue 7, July 2007. Page(s): 1430 – 1469

[3] Zou, W.Y and Yiyan Wu. "COFDM: an overview". *IEEE Transactions on Broadcasting,* Volume 41, Issue 1, March 1995 Page(s):1 - 8 .

[4] M. O'Droma and Mgebrishvili, N. "On quantifying the benefits of SSPA linearization in UWC-136 systems". *IEEE Transactions on Signal Processing*. Volume 53, Issue 7, July 2005 Page(s): 2470 – 2476

[5] Hongwei Yang. "A road to future broadband wireless access: MIMO-OFDM-Based air interface". *IEEE Communications Magazine*, Volume 43, Issue 1, Jan. 2005, Page(s): 53 – 60

[6] Fager. C, Pedro. J.C, de Carvalho N.B, Zirath. H, Fortes. F, and Rosario, M.J. "A comprehensive analysis of IMD behavior in RF CMOS power amplifiers". *IEEE Journal of Solid-State Circuits*. Volume 39, No. 1, Jan. 2004, Page(s):24 – 34

[7] Wireless LAN Medium Access Control (MAC) and Physical Layer (PHY) specifications, IEEE Std 802.11a, 1999

[8] E. Bertran, M. O'Droma, P. Gilabert, and G. Montoro. "Performance Analysis of Power Amplifier Back-off Levels in UWB Transmitters". *IEEE Transactions on Consumer Electronics*, Volume 53, Issue 4, Nov. 2007, Page(s): 1309 – 1313

[9] Pedro, J.C, Garcia, J.A, and Cabral, P.M. "Nonlinear Distortion Analysis of Polar Transmitters". *IEEE Transactions on Microwave Theory and Thecniques.* Volume 55, No. 12, Dec. 2007, Page(s):2757 – 2765

[10] M. O'Droma. "Dynamic range and other fundamentals of the complex Bessel function series approximation model for memoryless nonlinear devices". *IEEE Transactions on Communications*. Volume 37, Issue 4, April 1989 Page(s): 397 – 398

[11] Minkoff. J. "The role of AM-PM conversion in memoryless nonlinear systems". *IEEE Transactions on Communications*. Vol.com 33, Issue.2, Feb 1985, Page(s): 139-144.

[12] M. O'Droma, N. Mgebrishvili, and A. Goacher. "New percentage linearization measures of the degree of linearization of HPA nonlinearity," *IEEE Commununications Letters,* Volume 8, Issue 4, April 2004 Page(s): 214-216

[13] M. O'Droma and Y. Lei. " A Novel Optimization Method for Nonlinear Bessel-Fourier PA Model Using an Adjusted Instantaneous Voltage Transfer Characteristic" in *38th European Microwave Conference*. Amsterdam Netherland, Octorber 2008.

[14] M. O'Droma and N. Mgebrishvili. "Signal Modeling Classes for Linearized OFDM SSPA Behavioral Analysis ". *IEEE Communications Letters.* Volume 9, Issue, Feb 2005, Page(s): 127-129